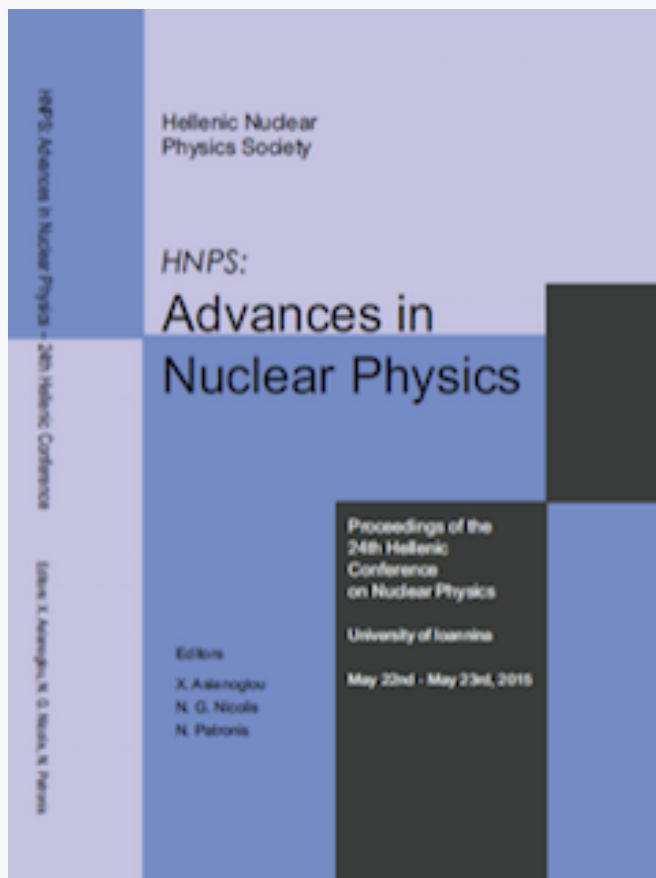


## HNPS Advances in Nuclear Physics

Vol 23 (2015)

HNPS2015



### Analysis of uncertainties associated with different factors used to determine the age of sediments with the Optically Stimulated Luminescence method

*I. M. Tsodoulos, K. Stamoulis, C. A. Papachristodoulou, K. G. Ioannides*

doi: [10.12681/hnps.1895](https://doi.org/10.12681/hnps.1895)

#### To cite this article:

Tsodoulos, I. M., Stamoulis, K., Papachristodoulou, C. A., & Ioannides, K. G. (2019). Analysis of uncertainties associated with different factors used to determine the age of sediments with the Optically Stimulated Luminescence method. *HNPS Advances in Nuclear Physics*, 23, 154–158. <https://doi.org/10.12681/hnps.1895>

## **Analysis of uncertainties associated with different factors used to determine the age of sediments with the Optically Stimulated Luminescence method**

I.M. Tsodoulos<sup>1</sup>, K. Stamoulis<sup>1,2</sup>, C. Papachristodoulou<sup>1</sup>, K. Ioannides<sup>1,2</sup>

<sup>1</sup> *Department of Physics, University of Ioannina, 45110, Ioannina, Greece.*

<sup>2</sup> *Archaeometry Center, University of Ioannina, 45110, Ioannina, Greece*

---

**Abstract** In this work, a sediment sample from an excavated paleoseismological trench was collected and dated following the Optically Stimulated Luminescence (OSL) dating method, using the Riso TL/OSL DA-20 reader. Chemically purified quartz, from the sample, was analysed following a single-aliquot regenerative-dose (SAR) protocol for the equivalent dose ( $D_e$ ) determination. Also, to estimate dose rates, the natural radioactivity of soil from the surroundings of the original sample location was measured, using gamma spectrometry. Since the application of the OSL dating method involves a number of intermediary factors and processes, all being the sources of uncertainties propagating to the total uncertainty, an exhaustive analysis of the involved uncertainties is presented and the implications to the derivation of the final ages are discussed.

**Keywords** Dose rate assessment, OSL dating method, uncertainty analysis.

---

### **INTRODUCTION**

The luminescence (Thermoluminescence-TL and Optically Stimulated Luminescence-OSL) dating methods depend on the accurate calculation of the accumulated radiation dose over a period of time (Equivalent Dose,  $D_e$ ) and the rate at which the material under study is exposed to dose due to environmental radiation (Dose Rate,  $D_R$ ).

Thus, when dating a sediment sample, two major sources of uncertainty ensue. One originates from the assessment of the equivalent dose through the OSL measurement's process [1]. The other comes from the assessment of  $^{40}\text{K}$ ,  $^{238}\text{U}$ ,  $^{235}\text{U}$ ,  $^{232}\text{Th}$  and daughter isotopes activities and also from the calculation of annual dose rates using the measured activities and is transferred to the age result [2]. Finally, the combination of the above uncertainties provides the uncertainty associated to the calculated age of the sample.

### **METHODS**

To elaborate on the uncertainties inherent in the luminescence dating methods, we proceeded through a worked example of dating a sediment sample (sample ID: Gyr1OSL\_08) taken from an excavated paleoseismological trench in the Gyrtioni area, Thessaly region, Greece. The paleoseismological trench was excavated perpendicular to the trace of the Gyrtioni Fault. The south facing Gyrtioni Fault is  $\sim 12$ -13 km long with ESE-WNW strike, at a distance of ca. 10 km from the city of Larissa [3]. The footwall of the fault consists of well stratified lagustrine deposits, while the hanging wall consists of poorly stratified fluvial and colluvial deposits. The interpretation of the trench wall structure provided indications of three surface faulting events.

The sample was collected with a metallic core sampler 15 cm long. The top content of the sampler was used to calculate the radioactivity of the surrounding sediment, while the rest was prepared for OSL measurements. The quartz grain fractions of 125–250  $\mu\text{m}$  were used, separated by dry sieving and aliquots were prepared using the standard laboratory preparation procedure [4]. The Single Aliquot Regenerative (SAR) protocol [5] was followed to measure the equivalent dose of twelve aliquots with a preheat temperature at 240  $^{\circ}\text{C}$  for 10 s, and a cut-heat of 160  $^{\circ}\text{C}$ . OSL signals were acquired at 125  $^{\circ}\text{C}$  for 40 s using blue light. Sample preparation and OSL measurements were conducted at the Archaeometry Center of the University of Ioannina.

The radioactivity of surrounding sediments was calculated analysing the major photopeaks of certain radioisotopes of the decay chains of  $^{238}\text{U}$ ,  $^{235}\text{U}$ ,  $^{232}\text{Th}$  and  $^{40}\text{K}$  (Fig. 1a). The sample was dried and passed through a 500  $\mu\text{m}$  sieve. Gamma spectrometry was conducted using a high-purity Broad Energy Germanium (BEGe) detector (Canberra  $\gamma$  detection system) (Fig. 1b). The OSL signal was measured using the Risø TL/OSL-DA-20 reader [6] (Fig. 1c).

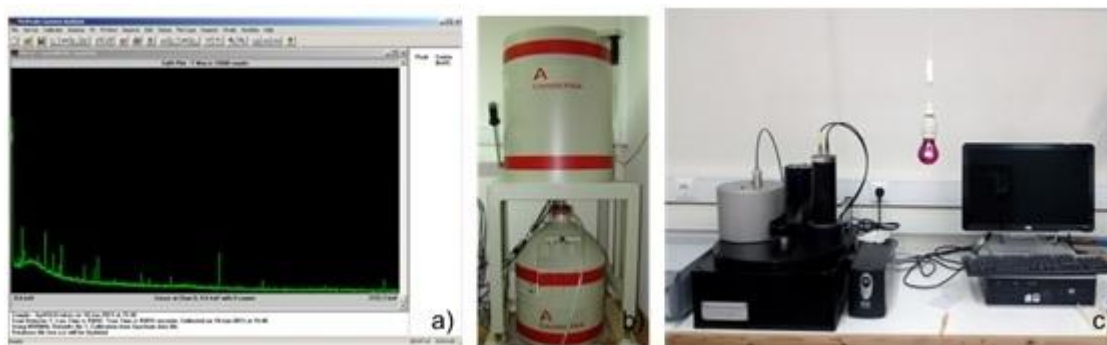


**Fig. 1.** a) The gamma-ray spectrum of Gyr1OSL\_08 sample, b) the high-purity Broad Energy Germanium (BEGe) detector and c) the Risø TL/OSL-DA-20 reader of the Archaeometry Center of the University of Ioannina.

## RESULTS AND DISCUSSION

Assesed values and accompanying uncertainties for each type of measurements are shown in the Tables 1 to 4. In Table 1, the relative uncertainties of the gamma spectrometry analysis of the selected sediment sample are presented, i.e. the gross and background counting rates of various isotopes together with the propagated relative uncertainty in the calculation of the net counting rates. The detector efficiency relative uncertainty is assumed to be constant at 4.9%. This value was estimated as a mean value of the uncertainties in the calculation of the counting efficiency of the photopeaks of a  $^{152}\text{Eu}$  standard solution used to calculate the efficiency of the detector as a function of energy (Fig. 2). The last column contains the total relative uncertainty derived from the other uncertainties using standard error propagation theory. The uncertainties that arise from the sample mass measurements and from the intensities of each photopeak are in the order of 0-4% and 2%, respectively.

In Table 2, the calculated activity concentrations and uncertainties ( $1\sigma$ ) for each isotope are presented in columns 2 and 3. In column 4 the relative uncertainty (%) is the weighted uncertainty in the cases when the mean value is calculated from two or three photo-peaks of the same radioisotope. The calculated values of activity concentrations are used to estimate the dose rate of energy delivered to quartz crystals.

Then by means of appropriate dose rate conversion factors [4,7], the total dose rate delivered to quartz can be calculated by adding the dose rates. The uncertainties of dose rates of the natural radionuclides decay chains and <sup>40</sup>K were calculated using error propagation theory and taking into account the uncertainties of the dose conversion factors and activities. The associated uncertainties of the dose conversion factors are low varying from 0.3 to 3.3% for beta radiation conversion factors and from 0.2 to 2.1% for gamma conversion factors [7]. Thus the errors in activity calculations of parent radionuclides of natural decay series and <sup>40</sup>K, which vary from 4.7 to 122%, dominate the final propagated error. However the overall uncertainty in the calculation of the total dose rate of the surrounding the samples sediments soil is reduced to 4.8% (Table 3).

| Isotopes    | keV    | Gross counting rate | Background counting rate | Net counting rate | Detector Efficiency | Total Uncertainty |
|-------------|--------|---------------------|--------------------------|-------------------|---------------------|-------------------|
| Pb210       | 46.8   | 20.1                | 29.7                     | 29.3              | 4.9                 | 29.7              |
| Th234       | 63.4   | 44.0                | 20.7                     | 80.8              | 4.9                 | 81.0              |
| Th234       | 93.5   | 13.9                | 11.0                     | 21.8              | 4.9                 | 22.3              |
| U235        | 144.1  | 86.0                | 42.1                     | 264.6             | 4.9                 | 187.1             |
| Ra226       | 186.3  | 16.0                | 8.9                      | 36.4              | 4.9                 | 99.4              |
| Pb212       | 238.7  | 4.7                 | 6.3                      | 6.2               | 4.9                 | 7.9               |
| Ra223+Rn219 | 269.8  | 64.0                | 25.0                     | 73.8              | 4.9                 | 158.7             |
| Pb214       | 295.3  | 8.7                 | 7.3                      | 13.4              | 4.9                 | 14.3              |
| Ac228       | 337.9  | 12.4                | 37.3                     | 13.8              | 4.9                 | 14.6              |
| Pb214       | 351.5  | 5.7                 | 4.2                      | 8.4               | 4.9                 | 9.8               |
| Tl208       | 510.5  | 20.0                | 4.6                      | 254.7             | 4.9                 | 254.7             |
| Tl208       | 582.3  | 9.0                 | 6.9                      | 14.6              | 4.9                 | 15.4              |
| Bi214       | 609.1  | 6.3                 | 3.4                      | 11.8              | 4.9                 | 12.8              |
| Bi212       | 726.9  | 26.9                | 21.3                     | 41.7              | 4.9                 | 42.0              |
| Ac228       | 910.8  | 13.0                | 12.2                     | 16.1              | 4.9                 | 16.9              |
| Ac228       | 966.7  | 20.0                | 21.4                     | 25.3              | 4.9                 | 25.8              |
| Pa234       | 1000.6 | 15.3                | 18.7                     | 284.6             | 4.9                 | 284.7             |
| Bi214       | 1120.0 | 15.0                | 6.3                      | 37.0              | 4.9                 | 37.3              |
| K40         | 1460.3 | 4.0                 | 4.1                      | 4.6               | 4.9                 | 6.7               |
| Bi214       | 1764.2 | 13.3                | 5.5                      | 37.2              | 4.9                 | 37.5              |
| Ra224       | 241.0  | 4.0                 | 20.4                     | 7.5               | 4.9                 | 9.5               |

**Table 1.** Relative uncertainties (%) of measurements of the various isotopes along with the total propagated uncertainty.

The final step to calculate the age of a sample is to estimate the amount of radiation that the sample has been exposed to since the event being dated (equivalent dose,  $D_e$ ). This is done: a) by measuring the natural OSL signal for each aliquot of the sample, b) creating the dose response curve for each measured aliquot and c) projecting the sensitivity corrected natural OSL signal onto the dose response curve to calculate the equivalent dose.

Table 4 shows the equivalent doses ( $D_e$ ) as calculated by the Analyst (version 4.10) software using the exponential function for the fit of the growth curve for each disk. In the associated uncertainty of  $D_e$ , the instrument error of 1.1% is included. The uncertainty varied from 1.6-2.7% for the  $D_e$  and from 5.1-5.5 % for the calculated ages. The last four lines of the table show the means and the weighted means of  $D_e$  and ages with the associated uncertainties. The weighted uncertainties are much lower if compared to the standard deviation values ( $\sigma$ ) also shown. The differences of the average and the weighted mean are inside  $1\sigma$  range. It is useful to point out that when using the weighted mean the uncertainty is about 1.5%. Much higher uncertainties are calculated when using simple average and standard deviation, about 28%. This point is very critical for the age determination. While the associated uncertainties in calculating the dose rates,  $D_e$  and ages for each disk do not exceed 5-6%, the variation of calculated ages from disk to disk raise the overall uncertainty of the finally accepted age of the sample to almost 30%, in our

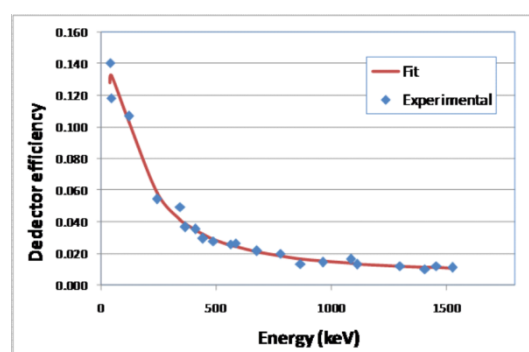


**Fig. 2.** Efficiency curve of the BEGe detector of the Archaeometry Center of the University of Ioannina.

example. This may be attributed to the incomplete bleach of the quartz grains when they are exposed to sun at the time of sedimentation.

| Isotopes | Activity concentrations (Bq/kg) | $\pm 1 \sigma$ | Uncertainty (%) |
|----------|---------------------------------|----------------|-----------------|
| Th234    | 14.6                            | 3.2            | 22.2            |
| Pa234    | 7.9                             | 22.4           | 284.7           |
| Ra226    | 16.5                            | 16.4           | 99.4            |
| Pb214    | 16.5                            | 1.3            | 8.1             |
| Bi214    | 14.8                            | 1.7            | 11.5            |
| Pb210    | 18.8                            | 5.6            | 29.7            |
| U235     | 0.4                             | 0.5            | 122.0           |
| Ac228    | 21.2                            | 1.7            | 8.1             |
| Ra224    | 26.1                            | 2.5            | 9.5             |
| Bi212    | 11.8                            | 4.9            | 42.0            |
| Pb212    | 18.2                            | 1.4            | 7.9             |
| Tl208    | 12.0                            | 1.8            | 15.4            |
| K40      | 442.8                           | 29.9           | 6.7             |

**Table 2.** Radioactivities and associated uncertainties of various isotopes.

| Equivalent Dose (Gy)      | $1\sigma$ | Uncertainty (%) | Age (ka) | $1\sigma$ | Uncertainty (%) |
|---------------------------|-----------|-----------------|----------|-----------|-----------------|
| 94.3                      | 1.5       | 1.59            | 53.0     | 2.7       | 5.08            |
| 117.0                     | 1.9       | 1.59            | 65.8     | 3.4       | 5.08            |
| 97.1                      | 1.6       | 1.60            | 54.6     | 2.8       | 5.08            |
| 76.2                      | 1.4       | 1.84            | 42.8     | 2.2       | 5.16            |
| 81.5                      | 1.5       | 1.86            | 45.8     | 2.4       | 5.17            |
| 76.5                      | 1.5       | 1.91            | 43.0     | 2.3       | 5.19            |
| 100.1                     | 1.8       | 1.79            | 56.2     | 2.9       | 5.14            |
| 88.2                      | 1.2       | 1.80            | 38.3     | 2.0       | 5.15            |
| 101.4                     | 1.8       | 1.81            | 57.0     | 2.9       | 5.15            |
| 135.7                     | 2.9       | 2.13            | 76.2     | 4.0       | 5.27            |
| 170.6                     | 4.6       | 2.72            | 95.8     | 5.3       | 5.53            |
| 102.4                     | 2.3       | 2.24            | 57.5     | 3.1       | 5.31            |
| <b>Mean</b>               | 101.7     |                 | 57.2     |           |                 |
| <b>Standard deviation</b> | 28.6      |                 | 16.1     |           |                 |
| <b>Weighted mean</b>      | 89.8      |                 | 50.8     |           |                 |
| <b>Weighted error</b>     | 0.5       |                 | 0.8      |           |                 |

**Table 4.** Equivalent doses ( $D_e$ ) and the calculated ages (ka) from 12 aliquots of Gyr1OSL\_08 sample.

|              | Decay chain activity |               | Dose rate    |               | Uncertainty (%) |
|--------------|----------------------|---------------|--------------|---------------|-----------------|
|              | Bq/kg                | $\pm 1\sigma$ | Gy/ka        | $\pm 1\sigma$ |                 |
| U238         | 15.8                 | 1.0           | 0.271        | 0.017         | 6.2             |
| U235         | 0.4                  | 0.5           | 0.001        | 0.002         | 122.0           |
| Th232        | 18.4                 | 0.9           | 0.282        | 0.013         | 4.7             |
| K40          | 442.8                | 29.9          | 1.231        | 0.083         | 6.7             |
| <b>Total</b> |                      |               | <b>1.805</b> | <b>0.086</b>  | <b>4.8</b>      |

**Table 3.** Radioactivities and calculated total dose rates from decay chains of  $^{238}\text{U}$ ,  $^{235}\text{U}$  and  $^{232}\text{Th}$  and for  $^{40}\text{K}$ . The overall dose rate is the sum of these dose rates and the associated uncertainty is calculated with error propagation theory.

## CONCLUSIONS

From the error analysis that was detailed above, it is evident that the major source of uncertainty in the age determination is the variability of the OSL signal measured in different aliquots of the same sample.

## ACKNOWLEDGEMENTS

This work is implemented within the framework of the Action «Supporting Postdoctoral Researchers» of the Operational Program "Education and Lifelong Learning" and is co-financed by the European Social Fund (ESF) and the Greek State.

## References

- [1] G.A.T. Duller, *Ancient TL* 25(1), p. 15-24 (2007)
- [2] S.M. Hossain et al, *Nuc. Inst. & Meth. In Phys. Res. A*490, (2002)
- [3] Caputo et al, *Geodin. Act.* 7(4), p. 219-231 (1994)
- [4] M.J. Aitken, *Oxf. Univ. Pr.*, p. 66 (1998)
- [5] Murray & Wintle, *Radiat. Meas.* 32(1), p. 57-73 (2000)
- [6] Bøtter-Jensen et al, *Radiat. Meas.* 45, p. 253-257 (2010)
- [7] Liritzis et al, *Medit. Arch. & Archaeom.* 12(3), p. 1-15 2013